

Supporting Information for “Precision-synthesis of supported metal nanoparticles: a solid-state chemical approach and the mechanistic understanding”

*Jianan Yu,^{a†} Tipaporn Patniboon,^{a†} Qingfeng Li,^a Søren Bredmose Simonsen,^a Thomas Willum Hansen,^b Pei Liu,^{*c} Heine Anton Hansen,^{*a} and Yang Hu ^{*a}*

^a Department of Energy Conversion and Storage, Technical University of Denmark, Fysikvej, 2800, Kgs. Lyngby, Denmark

^b DTU Nanolab, Technical University of Denmark, Fysikvej, 2800 Kgs. Lyngby, Denmark

^c Niels Bohr Institute, University of Copenhagen, Blegdamsvej 19, 2100 Copenhagen, Denmark

[†] These two authors contributed equally to this work.

SUPPLEMENTARY TABLE AND FIGURES

Table S1. Characteristic properties of synthesized samples.

Samples	Pt particle size (nm)	Pt loading (wt. %)	ECSA _{exp.} (m ² g _{Pt} ⁻¹)	ECSA _{actual} (m ² g _{Pt} ⁻¹)	ECSA _{theo.} (m ² g _{Pt} ⁻¹)	Weight content of particle (%)	Number of Pt particles (g ⁻¹)	Final particle size (nm)
PtN _x C _y @C	-	9.2	-	-	-	0	-	
H ₂ -600	1.2±0.2	10.9	16.1	23.4	230.8	10.1	5.65×10 ¹⁷	2.6
H ₂ -675	1.7±0.3	11.9	37.2	54.1	164.1	33.0	6.61×10 ¹⁷	2.5
H ₂ -700	2.1±0.2	12.0	40.3	58.6	131.3	44.6	4.66×10 ¹⁷	2.8
H ₂ -750	2.6±0.4	12.4	56.6	82.4	108.8	75.7	4.48×10 ¹⁷	2.8
H ₂ -850	2.7±0.4	13.5	70.1	101.9	102.8	99.2	5.03×10 ¹⁷	2.7
JM Pt/C	3.2±0.5	20.5	59.4	86.3	86.3	100	--	

Table S2. Element contents of synthesized Pt-based samples.

Samples	N, determined by XPS	N, determined by SEM-EDS	Pt, determined by SEM-EDS	
	(at. %)	(at. %)	(wt. %)	(wt. %)
PtN _x C _y @C	10.4	12.1	12.6	9.2
H ₂ -600	9.0	7.9	8.0	10.9
H ₂ -675	6.1	4.7	4.9	11.9
H ₂ -700	4.1	3.8	3.7	12.0
H ₂ -750	2.5	2.2	2.1	12.4
H ₂ -850	1.3	1.5	1.5	13.5

Table S3. Calculated atomic ratio of N/Pt_{SS} in synthesized samples.

Samples	Pt content	N content	Percentage of Pt single sites	N/Pt _{SS}
	(at. %)	(at. %)	(%)	atomic ratio
PtN _x C _y @C	0.6	12.1	100.0	-
H ₂ -600	0.7	7.9	89.9	12.4
H ₂ -675	0.7	4.7	67.0	9.5
H ₂ -700	0.9	3.8	55.4	8.0
H ₂ -750	0.9	2.2	24.3	10.5
H ₂ -850	0.9	1.5	-	-

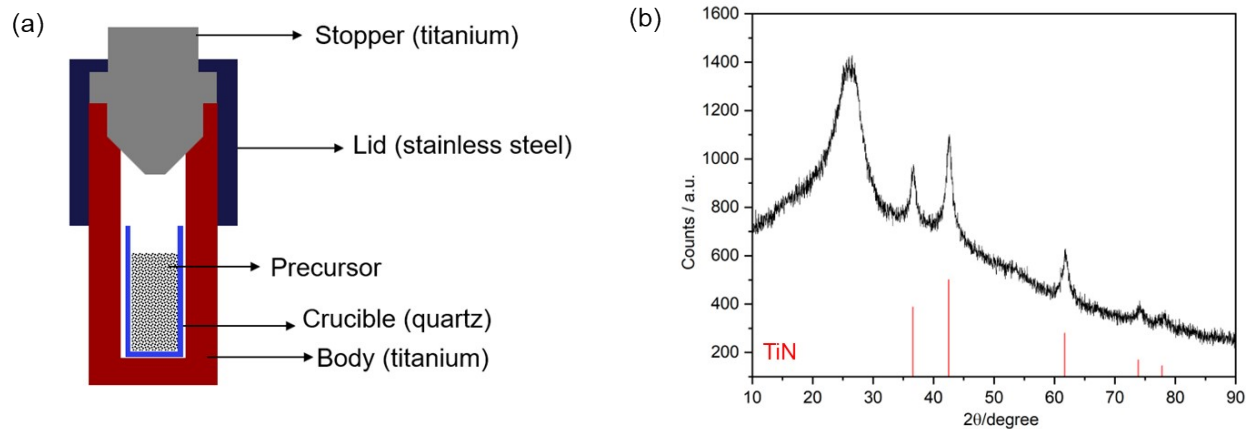


Figure S1. (a) Schematic illustration of the Ti autoclave. (b) XRD pattern of the sample directly attached to the inner wall the Ti autoclave after the synthesis at 800 °C, which reveals the presence of TiN (JCPDS: 65-5759).

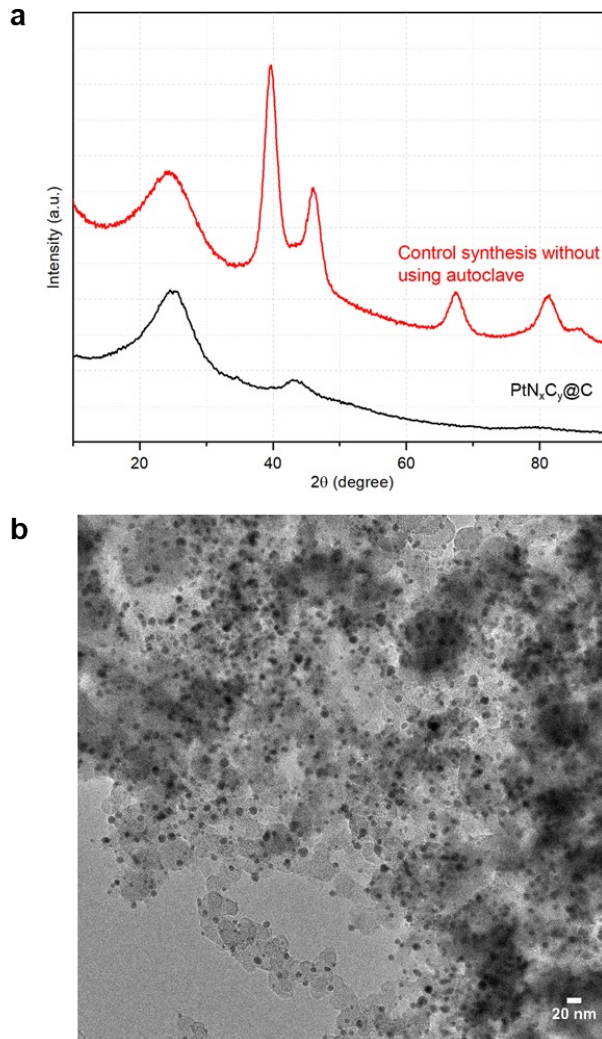


Figure S2. (a) XRD pattern of $\text{PtN}_x\text{C}_y@\text{C}$ in comparison to that of the sample synthesized without using the autoclave. (b) TEM images of Pd nanoparticles supported on Vulcan 72R carbon black, synthesized without using the autoclave for the first step.

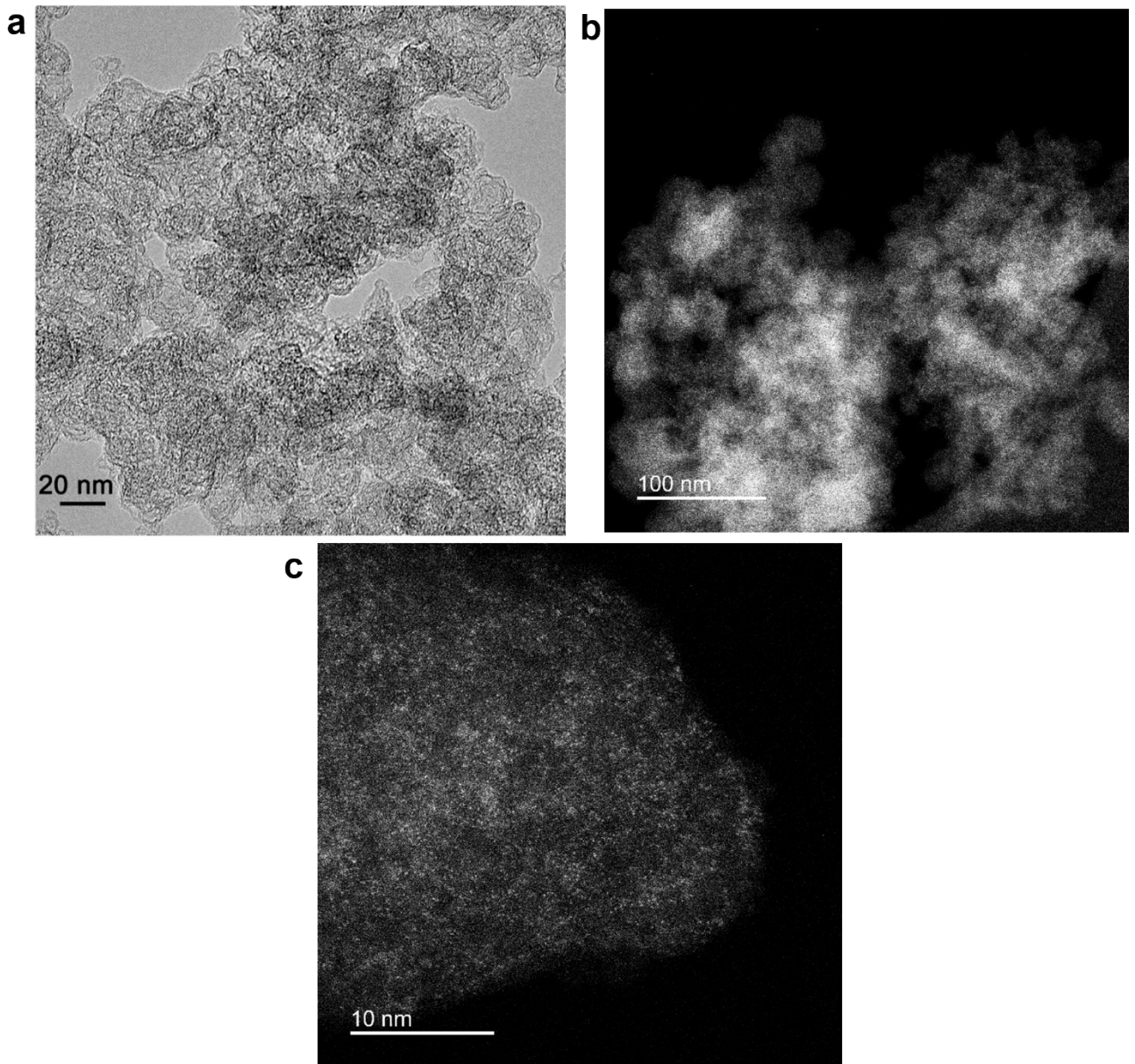


Figure S3. (a)TEM and (b,c) HAADF-STEM images of $\text{PtN}_x\text{C}_y@\text{C}$, which reveal the uniform distribution of single $\text{PtN}_x\text{C}_y@\text{C}$.

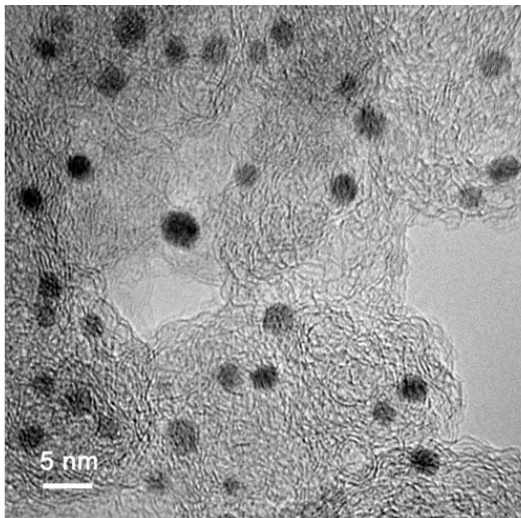


Figure S4. TEM image of H₂-850 sample, showing the formation of uniform Pt nanoparticles.

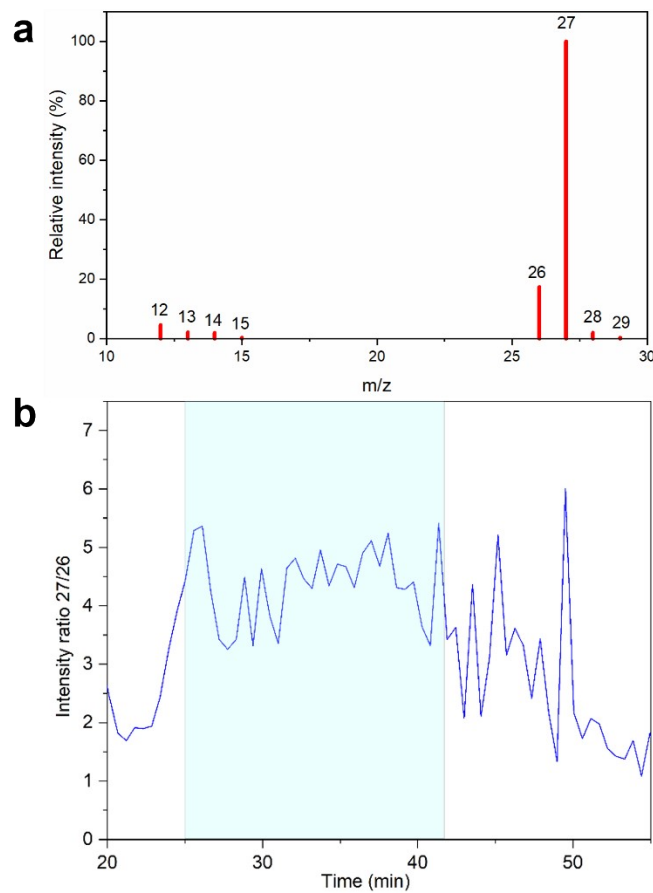


Figure S5. (a) Reference MS data of HCN from NIST Mass Spectrometry Data Center; (b) The intensity ratio of m/z 27 to m/z 26 throughout the process. The highlighted region indicates the time period with a significant amount of evolved gaseous products detected, same as that highlighted in Figure 2c.

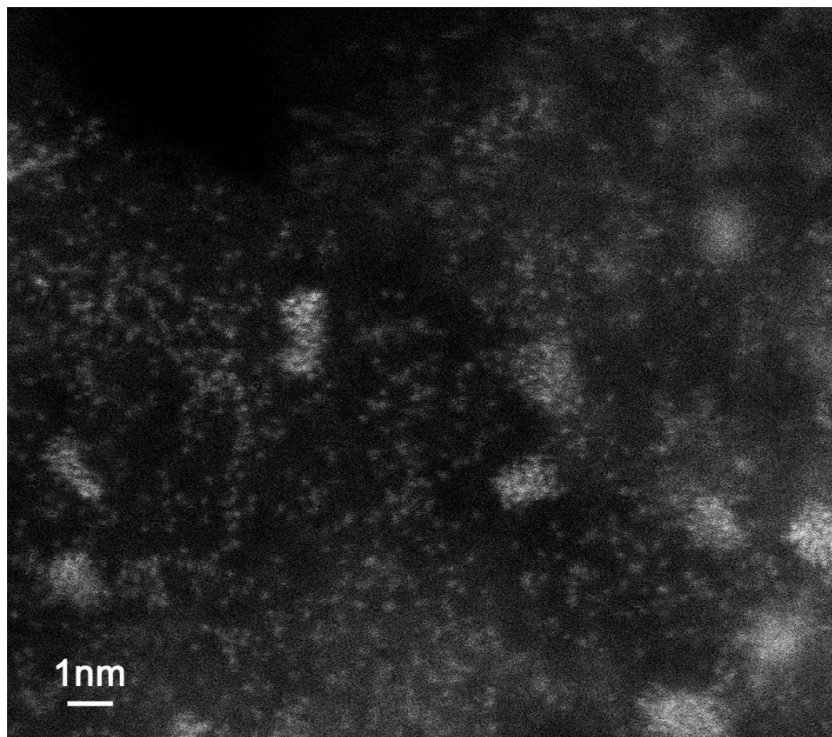


Figure S6. HAADF-STEM image of H₂-600, which reveals the disordered structures of the formed Pt nanoclusters.

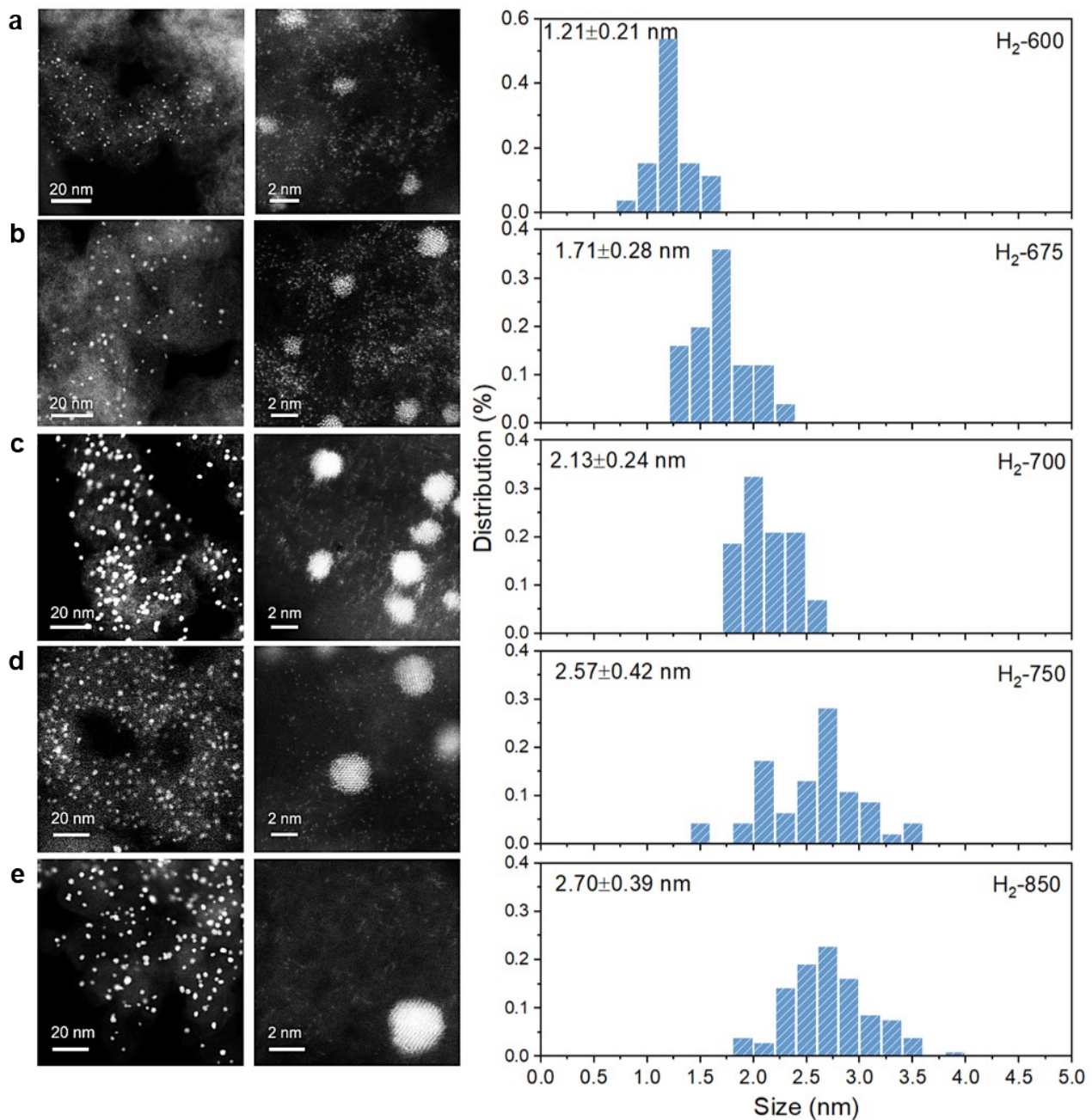


Figure S7. HAADF-STEM images of the series of samples synthesized at different reduction temperatures (left panels) and the corresponding histograms of the Pt particles (right panel), including (a) H₂-600, (b) H₂-675, (c) H₂-700, (d) H₂-750, and (e) H₂-850.

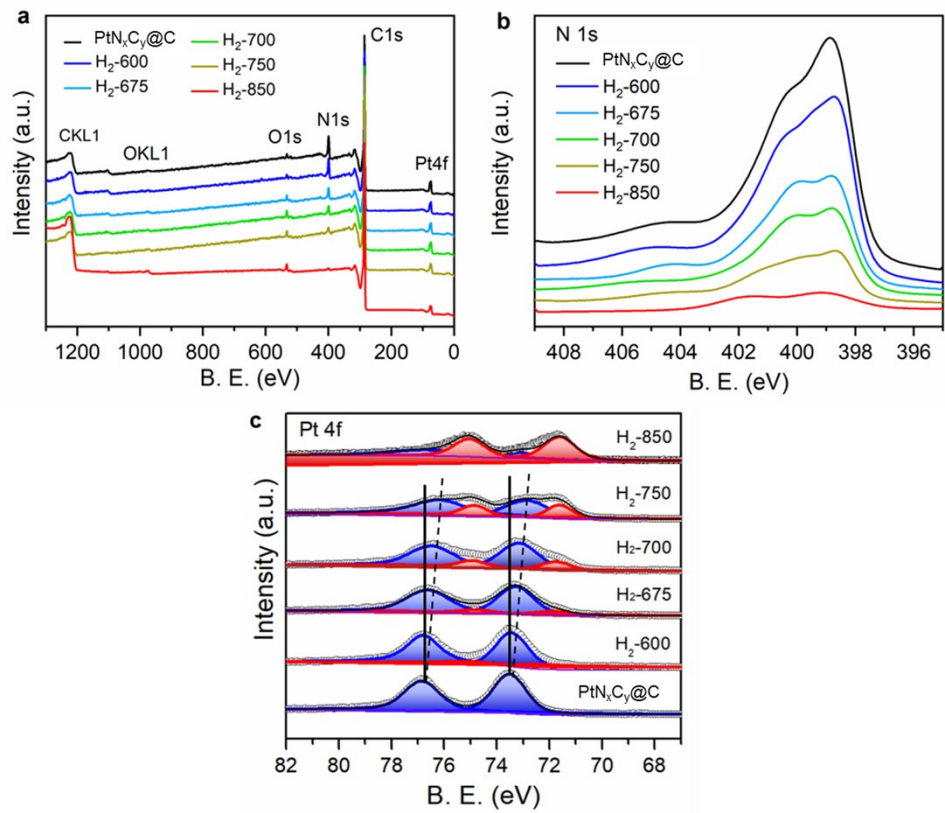


Figure S8. (a) XPS survey spectra, (b) narrow-scan N 1s spectra, and (c) narrow-scan Pt 4f spectra of the samples synthesized at different reduction temperatures.

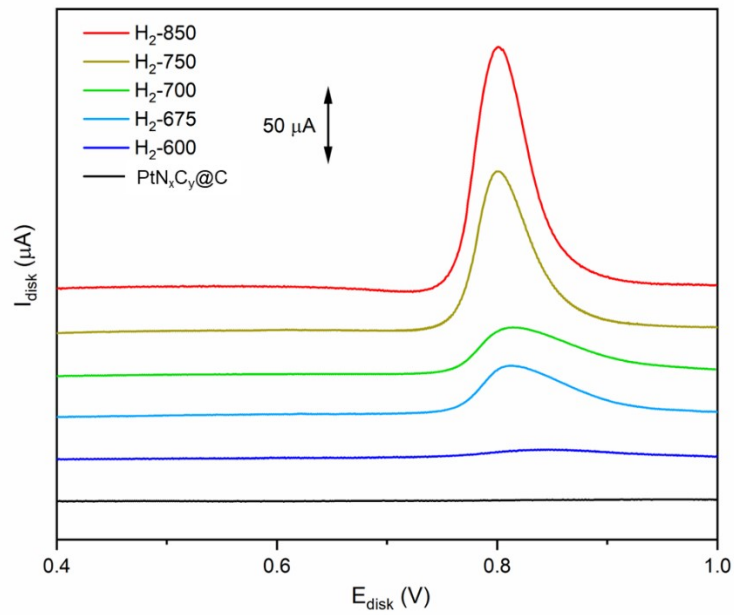


Figure S9. Normalized CO stripping peaks of the $\text{PtN}_x\text{C}_y@\text{sample}$ and the series of samples synthesized at different reduction temperatures.

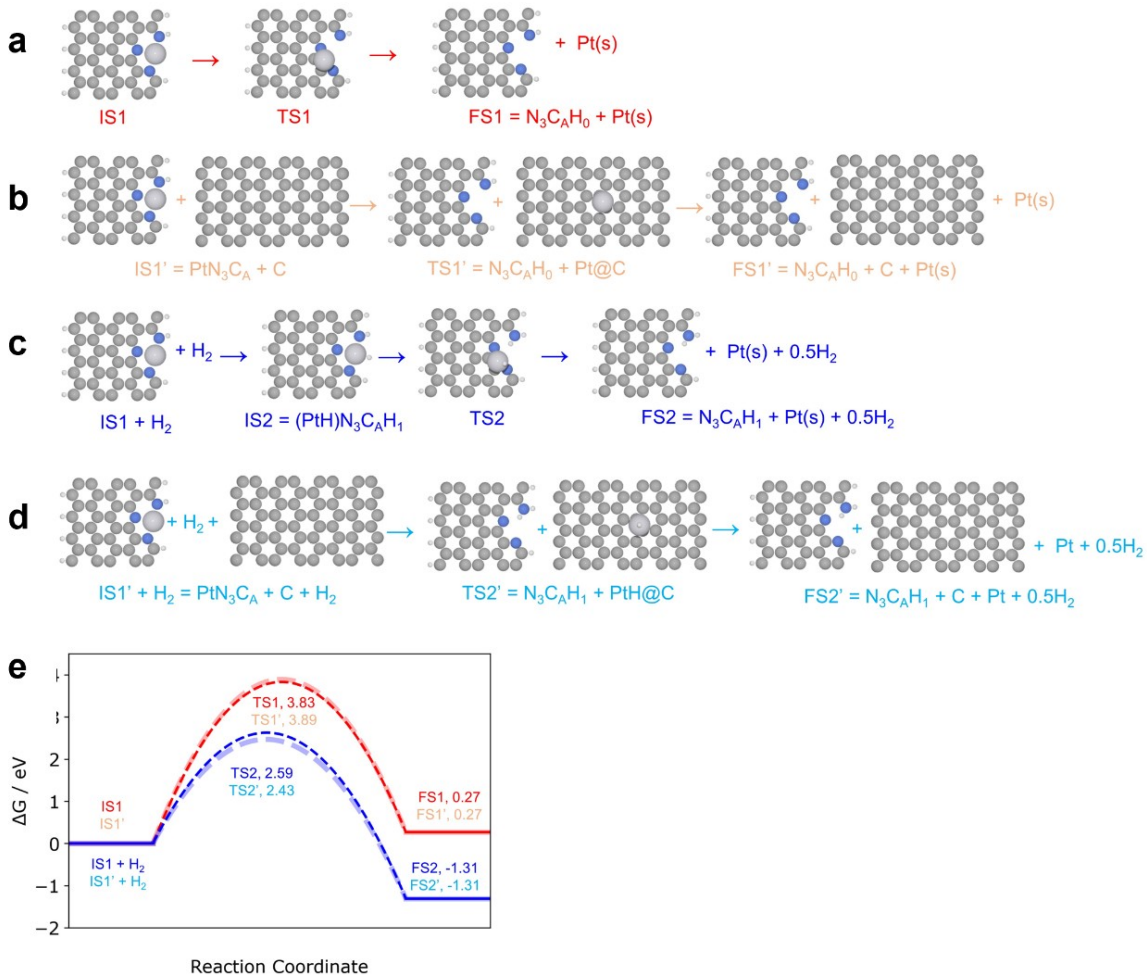


Figure S10. Stability of PtN_xC_y structures with and without H_2 at $T = 675^\circ\text{C}$ and $p(\text{H}_2) = 0.05$ bar.

Atomic structures illustrating the detachment of the Pt atom from the $\text{PtN}_3\text{C}_\text{A}$ structure without H_2

(a) TS1 from the NEB calculation and (b) TS1' from the approximation described in SI. The detachment processes with H_2 using (c) TS2 from the NEB calculation and (d) TS2' from the approximation. (d) Energy profiles for the detachment process with and without H_2 from the NEB calculation and the approximation. Colors of atoms: C = dark gray, Pt = light gray, N = blue, and H = white. Figure S10(a) shows the atomic structures for Pt atom detached from the $\text{PtN}_3\text{C}_\text{A}$

structure without H₂. TS1 was obtained from the CI-NEB calculation, and $\Delta E_a(TS1)$, which is the energy barrier obtained from the NEB calculation, can be calculated as

$$\Delta E_a(TS1) = E(TS1) - E(IS1) = E(TS1) - E(PtN₃C_A) = 3.83 \text{ eV}$$

where E(TS1) is the total energy of TS1 obtained from the NEB calculation. E(IS1) = E(PtN₃C_A) is the total energy of the PtN₃C_A structure. Figure S10b) shows the atomic structures for approximating the energy barrier of the same process. TS1' is the approximated structure for the transition state, and the approximated energy barrier is calculated as follows

$$\Delta E_a(TS1') = E(N₃C_AH₀) + E(Pt@C) - E(C) - E(PtN₃C_A) = 3.89 \text{ eV}$$

where E(N₃C_EH₀) is the total energy of the carbon cavity structure with 0 H atom binding at the carbon cavity. E(Pt@C) is the total energy of the isolated Pt atom on the (undoped) carbon surface, and E(C) is the total energy of the (undoped) carbon surface. From the energy profiles for the detachment process without H₂, as shown in Figure S10(e), it can be seen that $\Delta E_a(TS1) \approx \Delta E_a(TS1')$. The reaction free energy of the detachment without H₂ in both Figure S10(a) and S10(b) can be written as follows

$$\Delta G_R = E(Pt) + E(N₃C_AH₀) - E(PtN₃C_A)$$

where E(Pt) is the energy per atom of the Pt in the FCC structure

Similarly, Figure S10(c) shows the atomic structures for the single Pt atom detached from the PtN₃C_A structure in the presence of H₂. TS2 was obtained from a CI-NEB calculation, and $\Delta G_a(TS2)$, which is the kinetic free energy barrier obtained from the NEB calculation, can be calculated as

$$\begin{aligned} \Delta G_a(TS2) &= [E(TS2) - E(IS2)] + [G(IS2) - E(IS1) - G(H₂)] \\ &= [E(TS2) - E((PtH)N₃C_AH₁)] + [G((PtH)N₃C_AH₁) - E(PtN₃C_A) - G(H₂)] \\ &= 2.35 \text{ eV} \end{aligned}$$

where E(TS2) is the total energy of TS2 obtained from the NEB calculation. E(IS2) = E((PtH)N₃C_AH₁) is the total energy of the (PtH)N₃C_AH₁ structure. G(IS2) = G((PtH)N₃C_AH₁) is total free energy of the (PtH)N₃C_EH₁ structure (G = E + ZPE + U_{vib} - TS_{vib}). G(H₂) is the total free energy of a H₂ gas molecule (G = E + ZPE + H - TS). Figure S10(d) shows the atomic structures for approximating the energy barrier of the same process in the presence of H₂. TS2' is the approximated structure for the transition state and the approximated energy barrier is calculated as follows

$$\begin{aligned} \Delta G_a(TS2') &= [G(N₃C_AH₁) + G(PtH@C) - G((PtH)N₃C_AH₁)] + [G((PtH)N₃C_AH₁) - G(H₂) - E(C) - E(PtN₃C_F)] \\ &= G(N₃C_AH₁) + G(PtH@C) - G(H₂) - E(C) - E(PtN₃C_A) \\ &= 2.19 \text{ eV} \end{aligned}$$

where $G(N_3C_AH_1)$ is the total free energy of the total energy of the carbon cavity structure with one H atom. $G(PtH@C)$ is the total free energy of the isolated Pt atom with 1H adsorbate on the carbon surface. We also find $\Delta G_a(TS2) \approx \Delta G_a(TS2')$ for the detachment with H_2 . The reaction free energy of the detachment with H_2 in both Figure S10(c) and S10(d) can be written as follows.

$$\begin{aligned}\Delta G_R &= E(Pt) + G(N_3C_AH_1) + 0.5 G(H_2) - E(PtN_3C_A) - G(H_2) \\ &= E(Pt) + G(N_3C_AH_1) - E(PtN_3C_A) - 0.5G(H_2)\end{aligned}$$

We can approximate the kinetic barrier for the detachment with and without H_2 by considering the thermodynamic energy difference. For the other considered PtN_xC_y structures in Figure S13, the energy barriers for the detachment with and without H_2 are approximated from the following thermodynamic calculations.

The approximated energy barrier for the detachments of a single Pt atom from the PtN_xC_y site without H_2 ($n = 0$ where n is the number of H atoms binding at the carbon cavity structure) can be generally written as

$$\Delta G_a(n=0) = E(N_xCH_{n=0}) + E(Pt@C) - E(C) - E(PtN_xC) + \Delta TS_{\text{diffuse}}$$

The approximated energy barrier for the detachment of a single Pt atom from the PtN_xC site with H_2 can be generally written as follows ($n > 0$ where n is the number of H atoms binding at the carbon cavity structure).

$$\Delta G_a(n>0) = G(N_xCH_{n>0}) + G(PtH@C) - 0.5(n+1)G(H_2) - E(C) - E(PtN_xC) + \Delta TS_{\text{diffuse}}$$

where $\Delta TS_{\text{diffuse}}$ ($= 0.15$ eV) and $\Delta TS_{\text{diffuse}H}$ ($= 0.08$ eV) is the diffusion energy barrier for the isolated Pt atom and isolated Pt atom with one H adsorbate on the carbon surface. We include the diffusion barrier for the isolated PtH (Pt) on the carbon surface in the approximated energy barrier as we consider that the isolated Pt atom after the detachment is possibly on a carbon surface, diffusing around and agglomerating to form a Pt cluster. The N-dopant atoms and defects on the carbon surface can affect the diffusion energy barrier of the isolated Pt (PtH) atom (possibly increasing the energy barrier). The calculated energies reported here are a lower limit for the energy barrier.

The half-life ($t_{1/2}$ in s unit) for the PtN_xC site can be approximated as follows

$$k = (k_B T / h) \exp(\Delta G_a(n > 0) / k_B T) \text{ and } t_{1/2} = k^{-1}$$

where k_B is the Boltzmann's constant (in eV/K), h is Planck's constant (in eV s), and T is the temperature (in K). While the $t_{1/2}$ gives information about the rate of the detachment, the reaction free energy for the detachment tells whether the detachment is thermodynamically favorable, and it can be generally calculated as follows (n is the number of H atoms binding at the carbon cavity structure).

$$\Delta G_R(n \geq 0) = E(Pt) + G(N_xCH_{n \geq 0}) - E(PtN_xC) - 0.5nG(H_2); n \geq 0$$

where $E(Pt)$ is the energy per atom of the Pt in its FCC structure, and due to the cohesion energy in its bulk structure, the calculated energies reported here are a lower limit for the free reaction energy of nanoparticle formation.

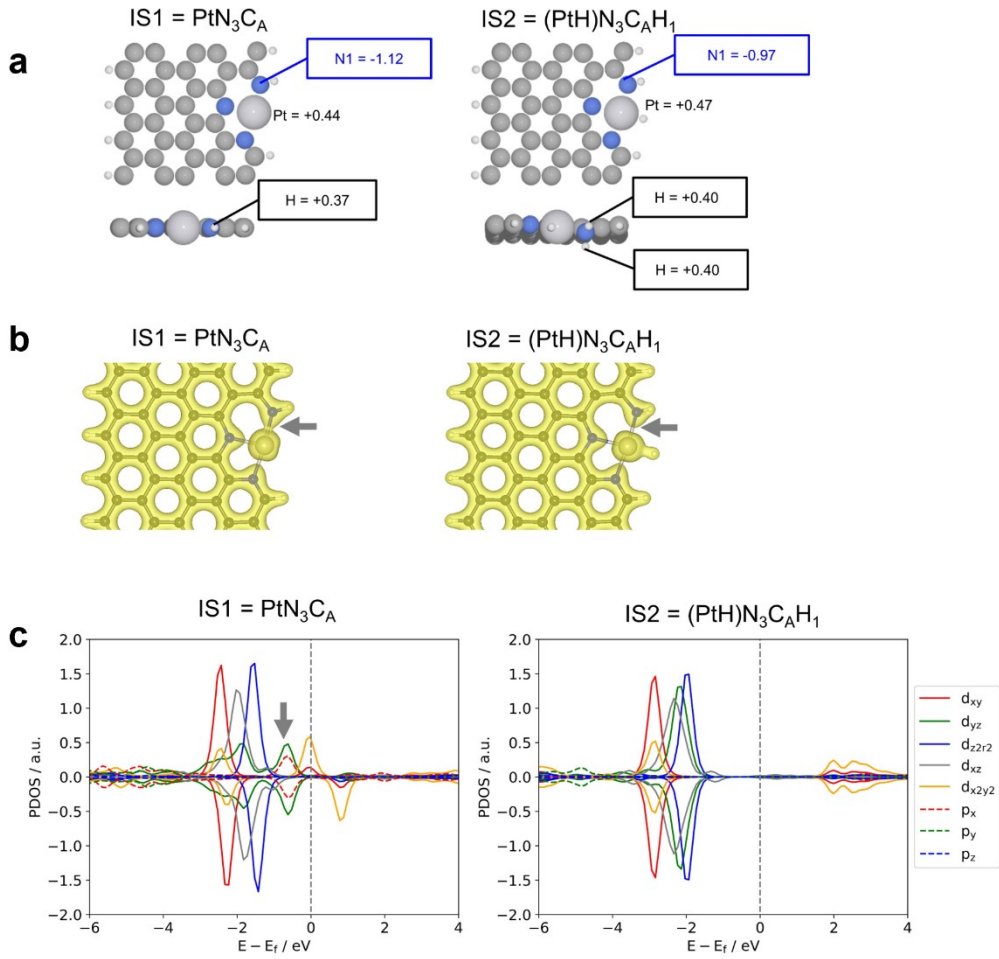


Figure S11: The detachment of a single Pt atom from the PtN_3C_A structure. (a) Atomic structure and Bader charge ¹ on atoms, (b) isosurface charge density (at isosurface level = 0.12 electron/ \AA^3), and (c) project density of states (PDOS) on the Pt atom (d-orbitals in solid lines), and N1 atom (p-orbitals in dashed lines) in IS1 = PtN_3C_A and IS2 = $(\text{PtH})\text{N}_3\text{C}_A\text{H}_1$ structure. Colors of atoms: C = dark gray, Pt = light gray, N = blue, and H = white.

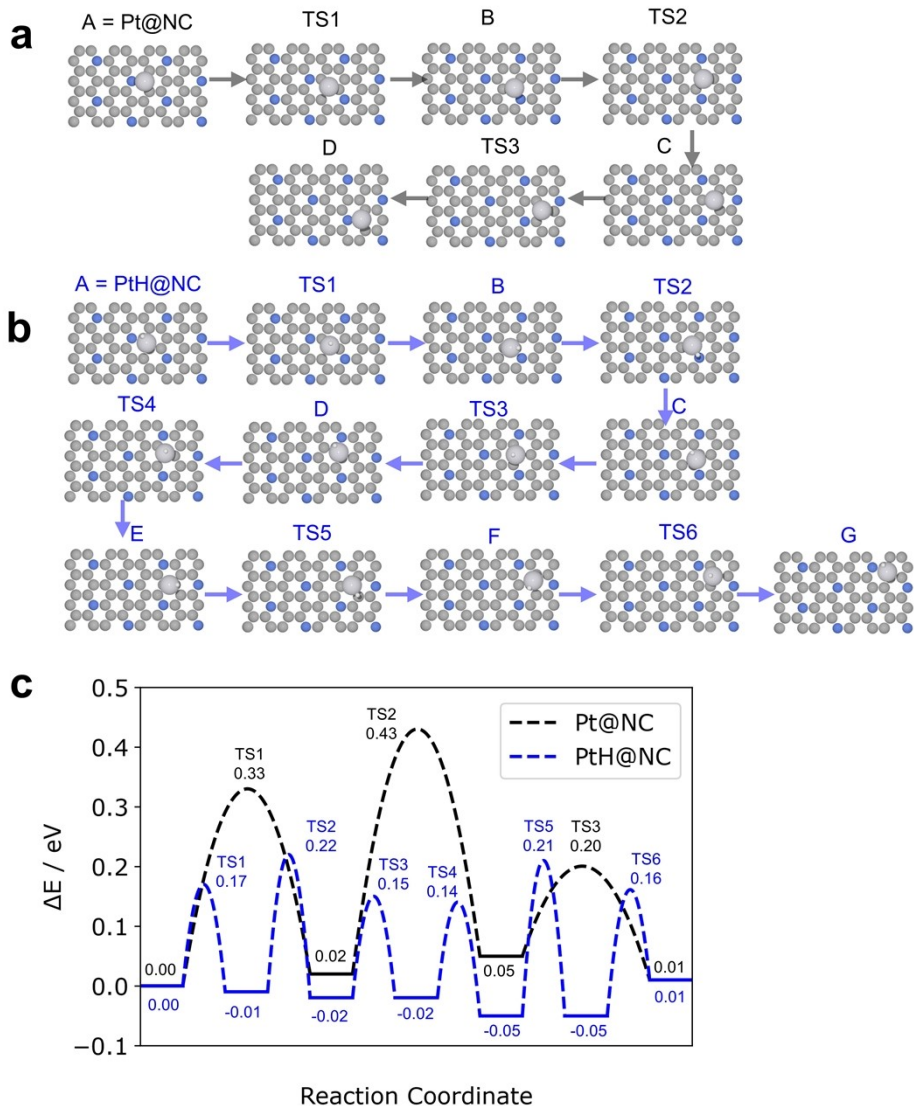


Figure S12. The diffusion of an isolated Pt atom on an N-doped carbon surface. Atomic structures illustrating the diffusion of (a) the isolated Pt atom and (b) the isolated Pt atom with an H adsorbate (PtH) on an N-doped carbon surface. (c) Energy profiles for the diffusion of the Pt@C (black line) and the PtH@C (blue line) on the N-doped carbon surface. Colors of atoms: C = dark gray, Pt = light gray, N = blue, and H = white.

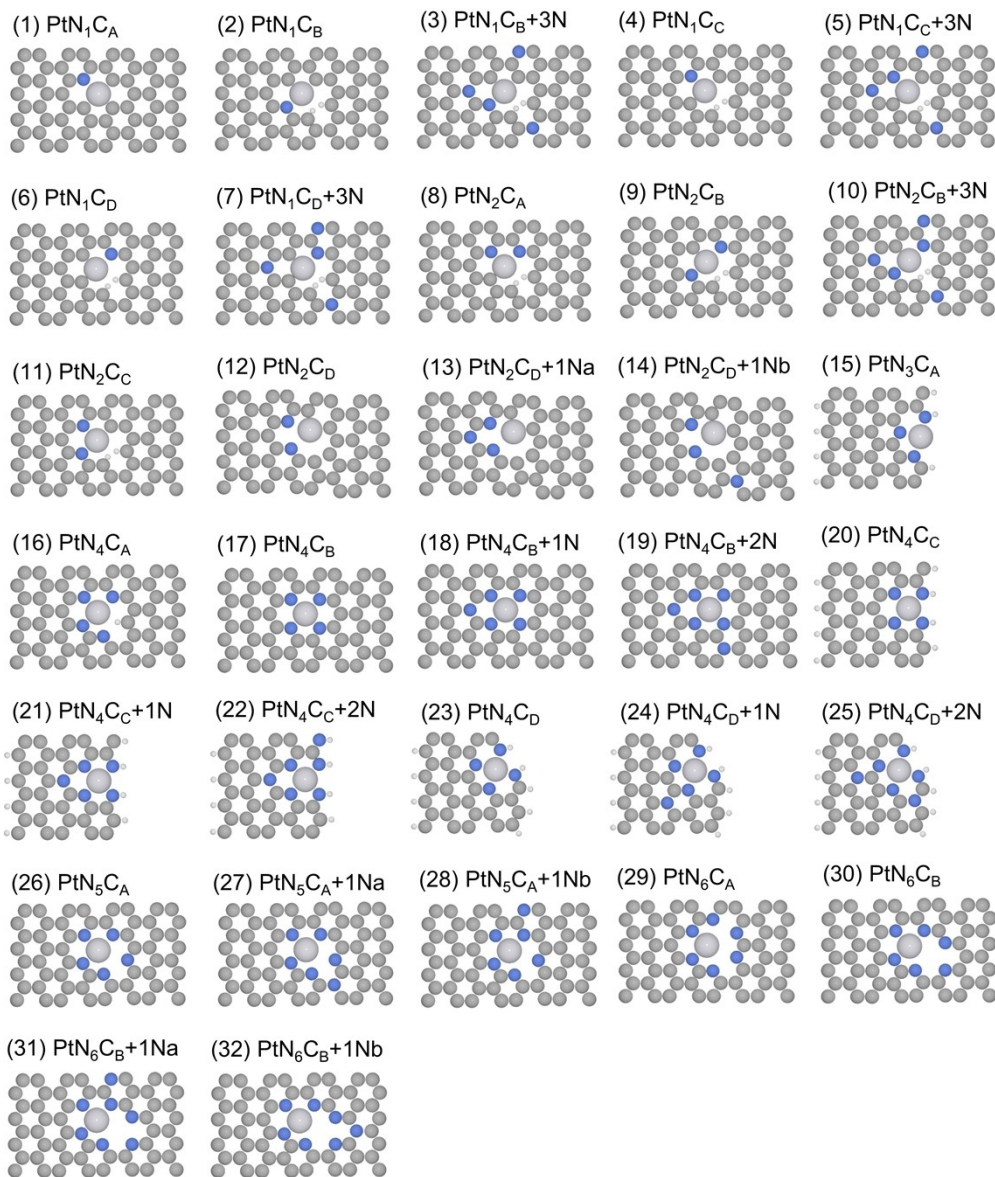


Figure S13. Structural models of PtN_xC_y considered in this study. Different PtN_xC_y motifs on the carbon surfaces are considered, where x denotes the number of N atoms coordinated with a single Pt atom in the PtN_x motifs ($x = 1-6$) and y denotes the different carbon surface ($y = \text{A}, \text{B}, \text{C}, \text{D}$). $\text{PtN}_x\text{C}_y+z\text{N}$ denotes PtN_xC_y motifs with z graphitic N atom around the motif. Colors of atoms: C = dark gray, Pt = light grey, N = blue, and H = white. Other possible Pt-N-C structures in the synthesized Pt-N-C@C sample that can transform into a Pt cluster need to satisfy two criteria: 1)

The Pt-N-C structures are thermodynamically stable under the synthesis condition (without H₂), and 2) they are thermodynamically unstable under the H₂ exposure. The detachment of the Pt atom from the Pt-N-C structures is considered at T = 675 °C and p(H₂) = 0.05 bar. Different PtN_xC motifs on the carbon surface are considered (where x is the number of N atoms coordinated with a single Pt atom in the PtN_xC motifs. We also include the effect of graphitic N doping around the coordinated site. Thus, the total amount of N (coordinated + doping) varies from 1.6% to 12.8% atomic concentration, which is approximated in the concentration range of N content in the synthesized Pt-N-C@C sample.

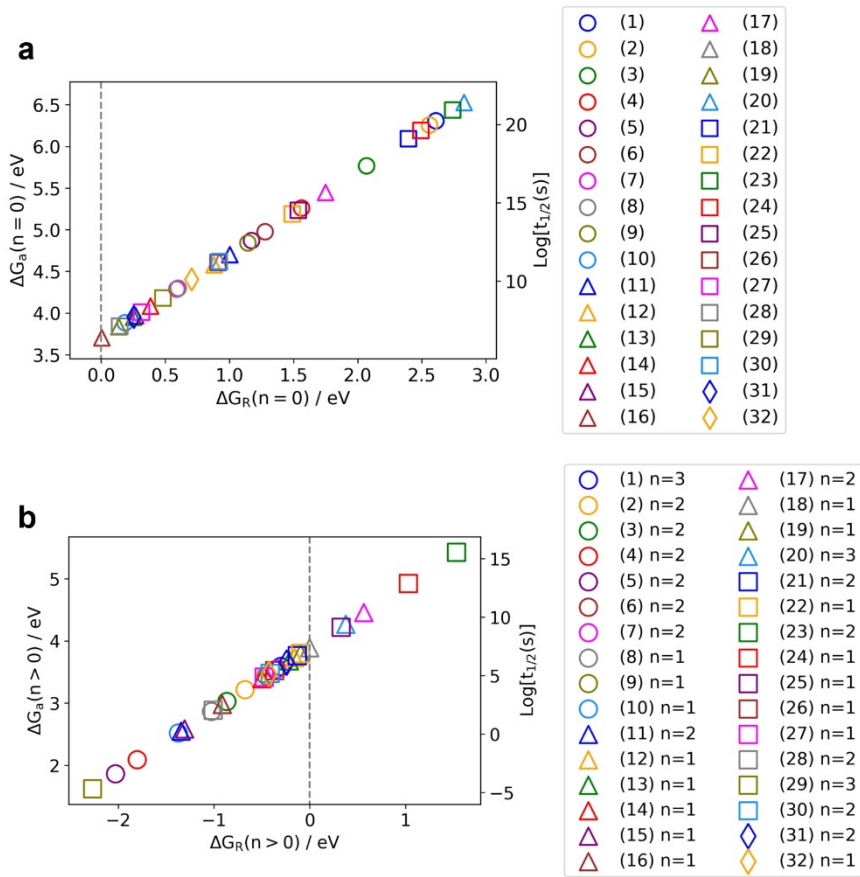


Figure S14. (a) $\Delta G_R(n=0)$ vs. $\Delta G_a(n=0)$ for detachment of a Pt atom from a PtN_xC_y structure without H_2 . (b) $\Delta G_R(n>0)$ vs. $\Delta G_a(n>0)$ for detachment of Pt atom from a PtN_xC_y structure in the presence of H_2 at $T = 675 \text{ }^\circ\text{C}$ and $p(\text{H}_2) = 0.05 \text{ bar}$. In Figure S15(b), n is the number of H atoms binding at the carbon cavity after removing the single Pt atom. Figure S15(b) shows only the n value that makes $\Delta G_R(n>0)$ most thermodynamically favorable for each PtN_xC_y structure. The considered structural models of the Pt-N-C structures are depicted in Figure S13.

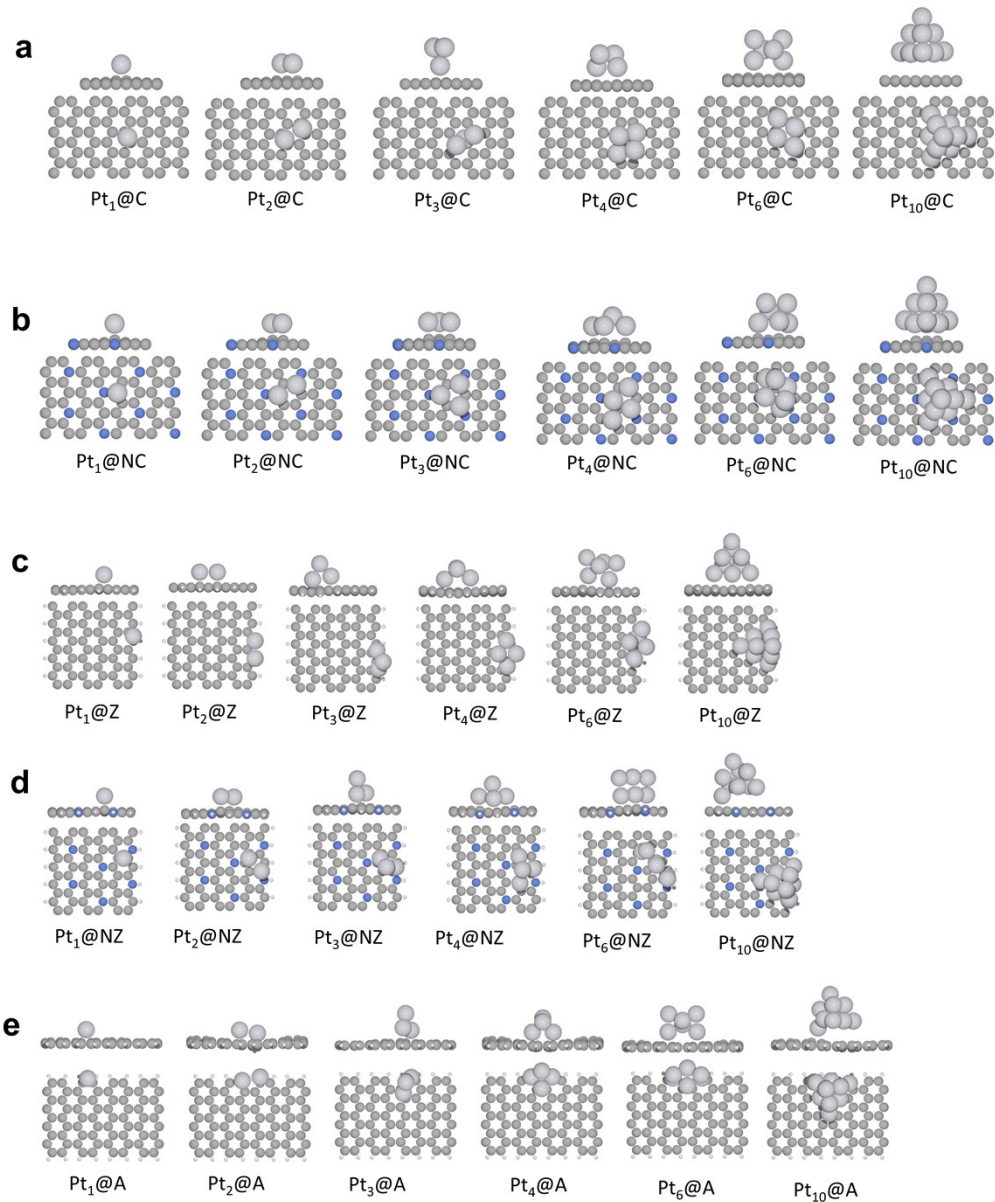


Figure S15. Nucleation of Pt clusters on different carbon surfaces. Atomic structures of Pt_m@X on: (a) C = undoped carbon surface, (b) NC = N-doped carbon surface, (c) Z = zigzag edge, (d) NZ = N-doped zigzag edge, (e) A = armchair edged. Color for atom: C = dark gray, Pt = light grey, N = blue, and H = white.

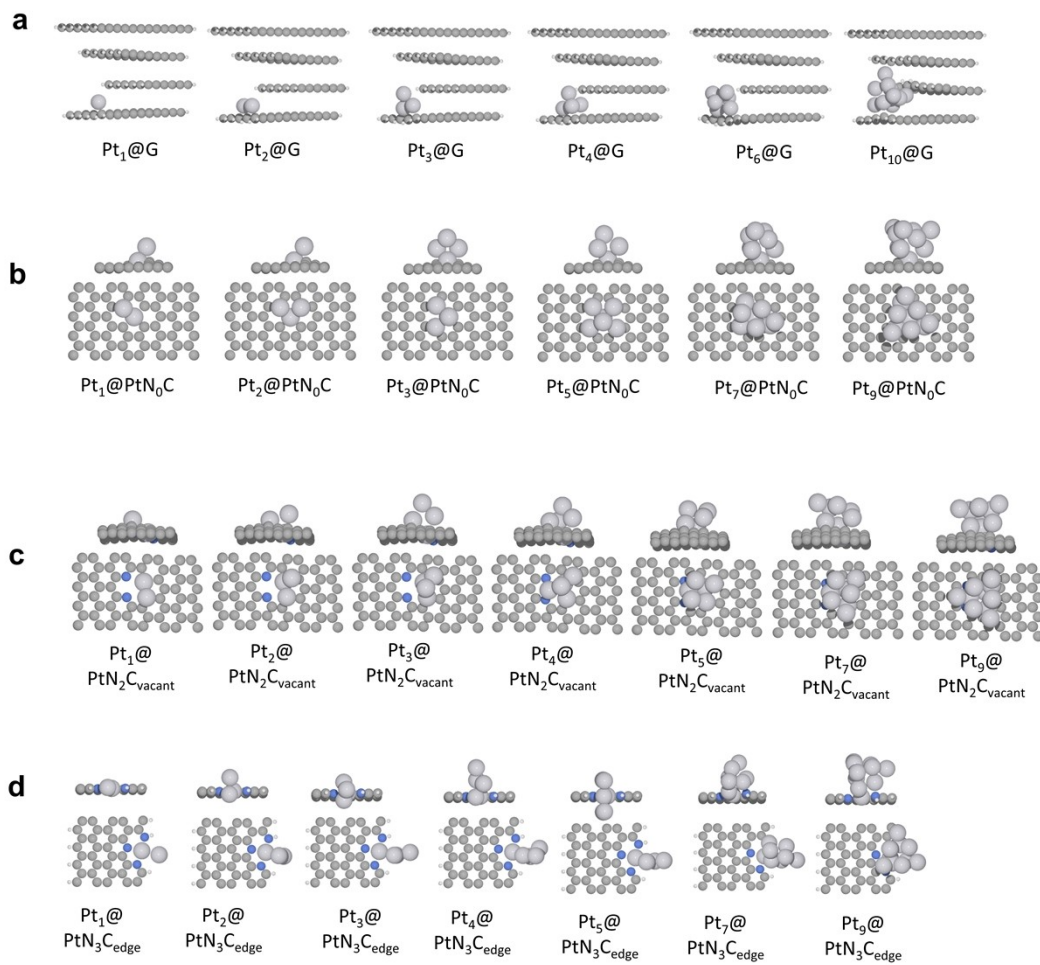


Figure S16. Nucleation of Pt clusters on different carbon surfaces. Atomic structure of Pt_m@X on: (a) G = graphite edge, (b) PtN₀C, (c) PtN₂C_{vacant} and (d) PtN₃C_{edge}, (e) A = armchair edged. Color for atom: C = dark gray, Pt = light grey, N = blue, and H = white.

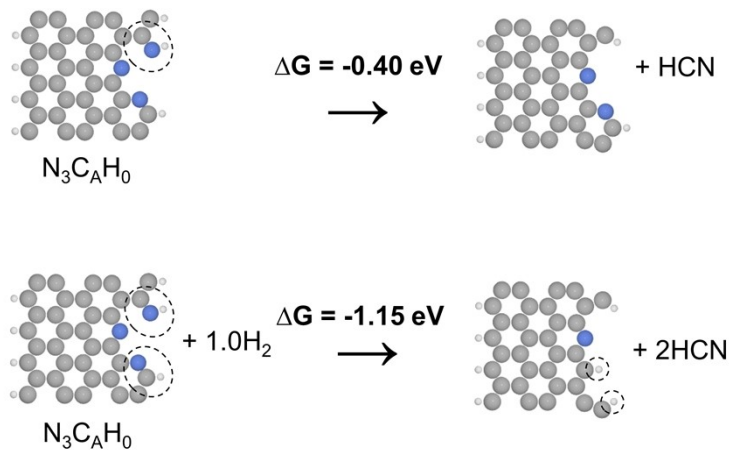


Figure S17. Formation of HCN. (a) Atomic structures illustrating possible formation pathways of HCN and corresponding reaction free energy at $T=675^\circ\text{C}$, $p(\text{H}_2)=0.05 \text{ bar}$, and $p(\text{HCN})= 1 \text{ mbar}$.

REFERENCES

1. W. Tang, E. Sanville and G. Henkelman, *Journal of Physics: Condensed Matter*, 2009, **21**, 084204.